Journal of Modern Optics
Publication details, including instructions for authors and subscription information:
http://www.tandfonline.com/loi/tmop20

Picosecond nonlinear optical studies of gold nanoparticles synthesised using coriander leaves (*Coriandrum sativum*)

S. Venugopal Rao [a]

[a] Advanced Centre of Research in High Energy Materials (ACRHEM), University of Hyderabad, Hyderabad 500046, India

Available online: 30 Jun 2011

To cite this article: S. Venugopal Rao (2011): Picosecond nonlinear optical studies of gold nanoparticles synthesised using coriander leaves (*Coriandrum sativum*), Journal of Modern Optics, 58:12, 1024-1029

To link to this article: http://dx.doi.org/10.1080/09500340.2011.590903

Journal of Modern Optics
Vol. 58, No. 12, 10 July 2011, 1024–1029

Taylor & Francis
Taylor & Francis Group

Picosecond nonlinear optical studies of gold nanoparticles synthesised using coriander leaves (*Coriandrum sativum*)

S. Venugopal Rao*

Advanced Centre of Research in High Energy Materials (ACRHEM), University of Hyderabad, Hyderabad 500046, India

(*Received 16 April 2011; final version received 16 May 2011*)

The results are presented from the experimental picosecond nonlinear optical (NLO) studies of gold nanoparticles synthesised using coriander leaf (*Coriandrum sativum*) extract. Nanoparticles with an average size of ~30 nm (distribution of 5–70 nm) were synthesised according to the procedure reported by Narayanan et al. [Mater. Lett. **2008,** *62,* 4588–4591]. NLO studies were carried out using the Z-scan technique using 2 ps pulses near 800 nm. Open-aperture data suggested saturation absorption as the nonlinear absorption mechanism, whereas closed-aperture data suggested a positive nonlinearity. The magnitude of third-order nonlinearity was estimated to be $(3.3 \pm 0.6) \times 10^{-13}$ esu. A solvent contribution to the nonlinearity was also identified and estimated. A comparison is attempted with some recently reported NLO studies of similar gold nanostructures.

Keywords: gold nanoparticle; nonlinear absorption; coriander leaves; Z-scan; picosecond

1. Introduction

Synthesis, physical, and optical characterisation of gold nanostructures in general, and gold nanoparticles (AuNP) in particular, has attracted extensive attention over the last decade due to their potential applications in a variety of fields, ranging from bio-sensing, drug delivery, and opto-electronics to cancer therapy [1–5]. Although a gamut of chemical synthesis methods exists for producing metal nanoparticles, the majority of the reactants and initial materials used in these reactions are toxic and potentially hazardous. Currently there is an escalating concern leading to the necessity for developing environmentally benign nanoparticles synthesis procedures that do not use toxic chemicals in protocols to avoid adverse environmental effects. Synthetic methods based on naturally occurring biomaterials provide an attractive alternative and environmental-friendly means. Recently, several groups have successfully achieved the synthesis of Ag, Au, and Pd nanoparticles using extracts obtained from unicellular organisms such as bacteria [6–9], fungi [10], and plant extracts [11–13]. Our group has been successful, through our recent experimental efforts, in synthesising silver nanoparticles using simple and bio-inspired method using the leaf broth of *Coriandrum sativum* and *Moringa oleifera*, for the first time, as both the reducing and stabilising agent [14,15]. Significantly, no other chemical reducing agent was used in the synthesis. The reaction was carried out in an aqueous solution and in a process that is benign to the environment. We had performed nonlinear optical (NLO) studies using nanosecond pulses and observed strong nonlinear optical coefficients and good optical limiting thresholds in both the cases. The NLO properties of diverse nanostructures, in general, and metallic nanoparticles, in particular, have been studied extensively due to the tremendous potential attached to them in biological imaging. The optical nonlinearity of nanomaterials varies with size, shape, distribution, host environment, etc., and rapid synthesis routes provide an excellent opportunity to understand and thereby control their physical, optical, and NLO properties [14–26]. Herein we present the picosecond (ps) nonlinear optical properties of gold nanoparticles near 800 nm studied with the Z-scan technique and synthesised using *Coriandrum sativum* (coriander; family Apiaceae) leaf extract [12]. Studies with ps or shorter pulses provide us with the necessary information on their figures of merit for all optical switching and optical signal processing applications.

2. Experimental

The procedure for synthesising AuNP was similar to the one reported recently [12]. Briefly, 20 g of fresh coriander leaves were washed thoroughly with double distilled water (DDW) and added to 100 ml of boiled sterile DDW for 5 min and filtered. The extract was

*Email: svrsp@uohyd.ernet.in

ISSN 0950–0340 print/ISSN 1362–3044 online

DOI: 10.1080/09500340.2011.590903
http://www.informaworld.com

stored at 4°C for further experiments. The filtrate was used as reducing and stabilising agent for 1 mM of $HAuCl_4$ (99.99%, Sigma-Aldrich). The leaf extract (1.5 ml) was added to 30 ml of 10^{-3} M $HAuCl_4$ aqueous solution and kept at 33°C. After 1 h the colour of solution changed from colourless to purple completely, indicating the formation of AuNP and the stabilisation was completed after three hours. The nanoparticles solution was collected and monitored by periodic sampling of aliquots (5 ml) of aqueous component and measuring the UV–visible spectra of solution.

Z-scan measurements [27] were performed using an amplified Ti:sapphire laser system (Legend, coherent) delivering nearly transform-limited pulses of ~2 ps (FWHM) and repetition rate of 1 kHz at 800 nm. The amplifier was seeded with ~15 fs (55–60 nm FWHM) pulses from an oscillator (Micra, coherent, ~1 W average power, 80 MHz repetition rate, 800 nm). Typically, laser pulses with 3–8 μJ energy were used for the experiments. The beam was focused using 200 mm focal length lens into the sample which was placed in 1 mm path length quartz/glass cuvettes. The beam waist at focus was estimated to be 30 ± 1 μm with a corresponding Raleigh range of 3.5 ± 0.2 mm. Typical peak intensities used for both closed- and open-aperture scans were in the $1–10 \times 10^{10}$ W/cm^2 range. The transmitted light was collected using a calibrated power meter and the sample movement was manually performed using a translation stage.

3. Results and discussion

Figure 1(*a*) shows the absorption spectra of AuNP solution monitored at different times. After three hours the colour change was permanent and absorbance of the nanoparticles remained constant. The peak near 536 nm in the absorption spectrum clearly confirms the formation of nanoparticles. Figure 1(*b*) shows a typical bright-field TEM micrograph of the synthesised AuNP. It is evident that most of the gold nanoparticles were spherical in shape, although triangular, truncated triangular, and decahedral morphologies along with some elongated nanoparticles were also observed [12]. The particle size varied from 5 to 70 nm and the average size was estimated to be ~30 nm. The slight differences in (a) time taken for nanoparticles formation, (b) particle distribution, and (c) the average size, compared to the earlier study [12], could be attributed to the quality of coriander leaves (key components) available in different places. The crystalline nature of AuNP was confirmed from the X-ray diffraction analysis. An FTIR spectrum recorded with freshly prepared solutions was similar to the reported spectrum [12]. We checked the reproducibility of the nanoparticles by synthesising them over a period of one week on a daily basis (with fresh coriander leaves solution prepared) and the results of absorption spectra combined with SEM data confirmed the formation of nanoparticles each time with similar results.

Figure 2(*a*) and (*b*) illustrate the closed-aperture data for AuNP 1 h 45 min (designated as solution A) and AuNP 3 h solutions (designated as solution B), respectively, recorded with a peak intensity of 25 GW/cm^2. Open triangles represent the experimental data, whereas the solid curves are theoretical fits. Open circles represent the data recorded for pure distilled water. The Z-scans were recorded for the pure coriander solution too and the data did not reveal any difference from the pure water curve. Therefore, we separated the contribution arising from the solvent and estimated the n_2 for AuNP to be $(6 \pm 1) \times 10^{-15}$ cm^2/W for solution A and $(7 \pm 1) \times 10^{-15}$ cm^2/W for solution B. To obtain the nonlinear absorption coefficient (β) the experimental data were fit to the

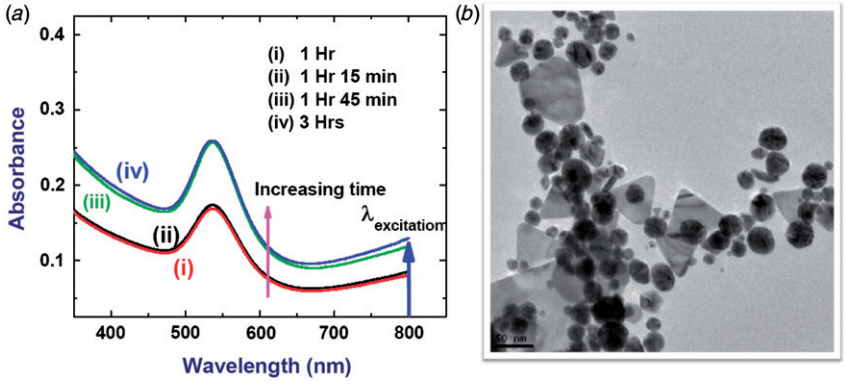

Figure 1. (*a*) Absorption spectra of the AuNP solution monitored at different times. Stable nanoparticles were formed after 3 h. (*b*) TEM image of the AuNP solution after 3 h. (The colour version of this figure is included in the online version of the journal.)

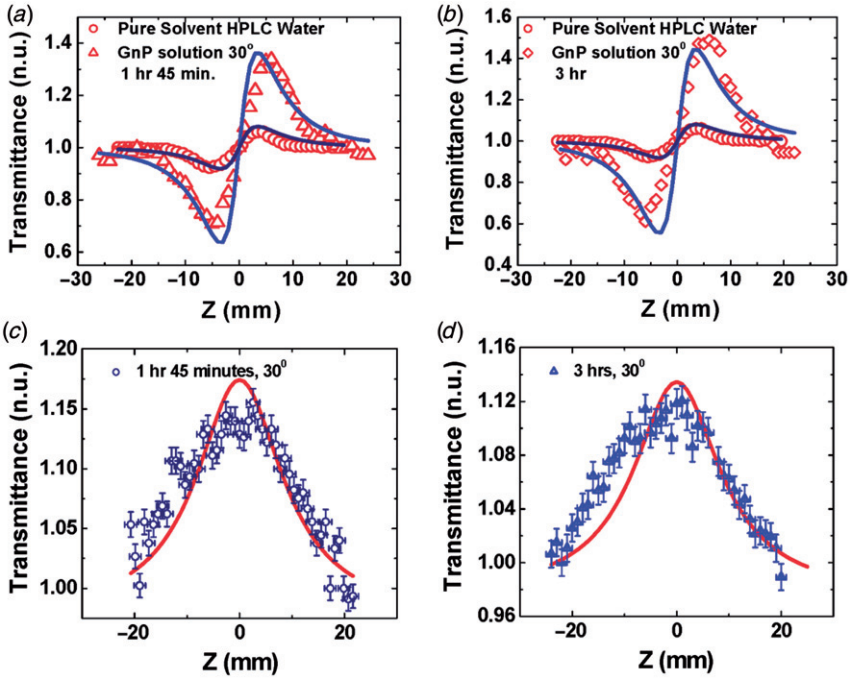

Figure 2. (*a*, *b*) Closed-aperture Z-scan data for 1 h 45 min and 3 h solution, respectively; (*c*, *d*) open-aperture data. (The colour version of this figure is included in the online version of the journal.)

expression for the normalised transmittance of an open aperture Z-scan [28]:

$$T_{OA(2PA)} = 1 - \frac{\beta I_0 L_{\text{eff}}}{2^{3/2}(1 + z^2/z_0^2)}, \qquad (1)$$

where z is the sample position, $z_0 = \pi\omega_0^2/\lambda$ is the Rayleigh range, ω_0 is beam waist at focus, λ is wavelength, I_0 is the peak intensity, and β is the nonlinear absorption coefficient. The effective optical path length is defined as $L_{\text{eff}} = \frac{1-\exp(-\alpha_0 L)}{\alpha_0}$, where α_0 is linear absorption coefficient.

Figure 2(*c*) and (*d*) depict the open-aperture scans for solutions A and B, respectively, recorded with a peak intensity of 50 GW/cm^2. It is evident that saturable absorption (SA) was mainly associated with a nonlinear absorption mechanism. Water and coriander leaves extract did not reveal any nonlinear absorption, as confirmed through separate open-aperture Z-scans. From the fits to experimental data (using Equation (1)) we estimated β to be 0.125 ± 0.02 cm/GW for solution A and 0.14 ± 0.02 cm/GW for solution B. The fitted values remained constant for measurements on solutions obtained after 3 h, again indicating the complete formation and stabilisation of nanoparticles. The values of real part, imaginary part, and total magnitude of $\chi^{(3)}$ were estimated from standard equations [28] to be $(3.0 \pm 0.5) \times 10^{-13}$ esu, $(6 \pm 0.9) \times 10^{-14}$ esu, and $(3.3 \pm 0.6) \times 10^{-13}$ esu, respectively. These values were obtained for solutions with 1 mM concentration. These values were reproducible, within the experimental errors, with synthesised samples from different batches (different days).

Figure 3 shows the open-aperture scans at higher peak intensities (>75 W/cm^2) and the behaviour clearly switched from SA to reverse SA (RSA) type near the focal region, which could be attributed to absorption from the higher excited states. The RSA obtained has been confirmed to be not from laser-induced damage of the nanoparticles by recording the absorption spectra before and after the Z-scan has been performed. Similar behaviour has also been observed by other groups [17]. This phenomenon is being investigated further. The measurements were repeated for the same solutions after one month and the nonlinear coefficients obtained were within the experimental errors, indicating the stability of the nanoparticles. We also confirmed the NLO coefficients obtained for nanoparticles achieved from different batches of synthesis were within the experimental errors mentioned above.

Several NLO studies [17–26,29–35] have been reported in the literature on different gold nanostructures and we attempt to compare these with the results obtained in this study (see Table 1). The absorption spectrum of AuNPs synthesised by us clearly demonstrates a low absorbance value at 800 nm. There is a possibility of a weak, second SPR peak appearance (probably due to the presence of few elongated

Table 1. Summary of the nonlinear coefficients from various studies in gold nanostructures.

Samples	Pulse details	Nonlinearity	Reference
Gold nanocubes (65 nm)	~60 fs, 800 nm	$\beta = 0.16$ cm/GW	[17]
Gold nanooctahedra (49 nm)		$\beta = 0.244$ cm/GW	
Gold nanoshells (60–100 nm)	~170 fs, 806 nm	$\beta = 0.03$–0.07 cm/GW	[18]
Gold nanospheres (~16 nm)	~15 ps, 450–750 nm	$\beta = 0.1$–0.7 cm/GW	[19]
Gold nanoparticles (70–170 nm)	~4 ns, 532 nm	$\beta = 0.152$ cm/GW	[20]
Gold nanoparticles (~3 nm)	~35 ps, 532 nm	saturable absorption	[21]
Gold nanorods (aspect ratio 3.8)	~220 fs, 800 nm	$\beta = 1.5$ cm/GW	[22]
Gold colloids (~12 nm)	~25 ps, 532 nm	$\beta = 10$ cm/GW	[23]
Silver nanoparticles (~26 nm)	~6 ns, 532 nm	$\beta = 72.5$ cm/GW	[14]
Gold nanostructures (~5 nm)	~35 ps, 532 nm	$\chi^3 \sim 2 \times 10^{-13}$ esu	[26]
Gold nanoparticles array (~16–18 nm height)	~50 fs, 800 nm	$\beta = 1300$ cm/GW	[33]
Gold nanoparticles array (160 nm, 300 nm, 600 nm, 820 nm)	~50 fs, 800 nm	$\beta = 0$–54 cm/GW	[34]
Gold nanoparticles in TiO_2	~40 ps, 1064 nm	$\chi^3 \sim 10^{-8}$ esu	[35]
Gold nanoparticles (~4 nm)	~35 ps, 1064 nm	Re $\chi^3 \sim 2 \times 10^{-13}$ esu $n_2 \sim 1.6 \times 10^{-14}$ cm^2/W	[27]
Oleylamine-capped gold nanoparticles (~7–10 nm)	~300 fs, 780 nm	$\beta = 0.097$ cm/GW	[29]
Gold nanoparticles (~30 nm)	~2 ps, 800 nm	$\beta = 0.14 \pm 0.02$ cm/GW $n_2 = (7 \pm 1) \times 10^{-15}$ cm^2/W Re $\chi^{(3)} = (3.2 \pm 0.5) \times 10^{-13}$ esu Im $\chi^{(3)} = (6 \pm 0.9) \times 10^{-14}$ esu $\chi^{(3)} = (3.3 \pm 0.6) \times 10^{-13}$ esu	This work

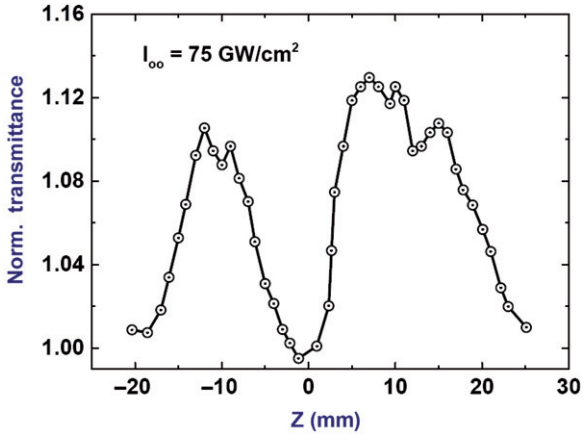

Figure 3. Open-aperture data of AuNP 3 h solution at a peak intensity of 75 GW/cm^2 indicating RSA within SA. (The colour version of this figure is included in the online version of the journal.)

nanoparticles) in the absorption spectrum for our AuNPs similar to the observations made by Elim et al. for their gold nanorods [22]. They detected a weak resonance at 800 nm in their gold nanorods and therefore observed SA which, changed into complete RSA at higher peak intensities. The observed SA behaviour in our case could be due to bleaching of the ground state surface plasmon band. Due to the limitations in our absorption spectrometer we could not record the spectra beyond 800 nm. Lee et al. [17] reported femtosecond NLO properties of gold nanocubes (65 nm) and nanooctahedra (49 nm) and observed SA with ~60 fs pulses (800 nm) at lower peak intensities (10–12 GW/cm^2) with magnitudes of 0.16 and 0.244 cm/GW. They argue that the 800 nm excitation is located at the edge of surface plasmon band of nanocubes and nanooctahedra. SA observed in their case was due to the bleaching of the ground state plasmon band, similar to our results. The slight differences in peak intensities where they observed RSA compared to ours lies in the shape and size distribution of the nanoparticles. Ros et al. [18] observed SA in gold nanoshells (60–100 nm) with 170 fs (806 nm) pulses and recorded a β value of 0.03–0.07 cm/GW. Boni et al. [19] observed SA type of nonlinear absorption and achieved a β value of 0.1–0.7 cm/GW for gold nanospheres (~16 nm) at different wavelengths (500–600 nm), some of which were close to resonance. Li et al. [20] studied gold nanoparticles (70–170 nm) functionalised with π-conjugated polymer using ns pulses and observed switching kind of behaviour within the SA signature of an open-aperture scan. They estimated β to be ~0.152 cm/GW along with the presence of higher nonlinearities. Reji et al. [21] studied gold nanoparticles (~3 nm) with 35 ps pulses (532 nm) and observed that ground-state plasmon bleach led to SA. Elim et al. [22] observed SA in gold nanorods (aspect ratio of 3.8) with ~220 fs

pulses and obtained β to be ~1.5 cm/GW. However, there was a second absorption peak at 800 nm for their elongated structures making that a resonant excitation study. Shen et al. [23] reported NLO studies on gold colloids (~12 nm) in polymer PVP and obtained a nonlinear coefficient of ~10 cm/GW. They too observed a positive nonlinearity as in our case. Though they used 25 ps pulses the excitation was at 532 nm, close to resonance, and the presence of polymer could have contributed to the high nonlinearity (10^{-10} esu) observed. Kai et al. [33] studied periodic triangular-shaped Au nanoparticles array fabricated on a quartz substrate using ~50 fs, 800 nm pulses and observed SA with different peak intensities. Wang et al. [34] demonstrated saturable absorption for larger size gold nanoparticles (70 nm, 140 nm, 190 nm sizes) array which switched to RSA for smaller sizes (37 nm) and argued that with large sized particles intraband contribution ascribed to the SA process becomes dominant though the absorbance at 800 nm was very weak. Cui et al. [35] also demonstrated SA behaviour for AuNP dispersed in TiO_2 thin films. Our recent studies [14] on silver nanoparticles synthesised using similar techniques resulted in a β value of ~72 cm/GW obtained with 6 ns pulses. Couris et al. [24] reported $\chi^{(3)}$ values for gold nanostructures (5 nm) in polymers to be $\sim 2 \times 10^{-13}$ esu examined with 35 ps pulses. Zhan et al. [27] estimated n_2 and Re $\chi^{(3)}$ of protected gold nanoparticles (~4 nm) to be -1.63×10^{-14} cm^2/W and -2.69×10^{-13} esu, respectively, with 35 ps pulses at 1064 nm. The negative sign obtained in their case could be attributed the distinctions in solvent used and the size of nanoparticles. Polavarapu et al. [29] studied the nonlinear optical properties of oleylamine-capped AuNP (~7–10 nm) using ~300 fs pulses near 780 nm and obtained a NLO coefficient β of ~0.07 cm/GW. Souza et al [30] reported n_2 values of $\sim 2.33 \times 10^{-14}$ cm^2/W for AuNP with sizes of $\sim 15 \pm 5$ nm (using ~200 fs, 800 nm pulses) for a fill factor of 23.1×10^{-5}.

From Table 1, which summarises the NLO measurements and coefficients obtained in various gold nanostructures, it is evident that the nonlinearity depends stringently on (i) pulse duration, (ii) wavelength of excitation, (iii) particle size, (iv) particle shape, and (v) the environment in which the particles are present. The values obtained with our AuNPs are comparable to those reported recently and there is scope for further improvement in improving/enhancing the nonlinearities through a systematic study involving the size and shape control. Our future studies will focus on (a) controlling the size/shape of these nanoparticles through use of different concentrations of the leaf extract, growth at different temperatures, and different environments, etc, (b) examining the performance of nonlinearity versus these physical properties, (c) stabilising these nanoparticles in a polymer matrix, and (d) nanosecond optical limiting [31,32] and femtosecond time-resolved studies to identify the potential of these molecules for optical limiting and switching applications in respective time domains.

4. Conclusions

In conclusion, we have studied the picosecond NLO properties of gold nanoparticles synthesised using coriander leaf extract. The solvent (distilled water) contribution was identified, estimated, and then decoupled from the overall magnitude of nonlinearity. A strong positive nonlinearity from the closed-aperture data and saturable absorption behaviour from the open-aperture data was inferred. The observed magnitude of nonlinearity was on par or better than some of the gold nanostructures studied recently.

Acknowledgements

S.V. Rao acknowledges the encouragement of Prof. Surya P. Tewari, ACRHEM and Prof. D. Narayana Rao, School of Physics. We also acknowledge the assistance of Dr Sathyavathi, School of Physics during synthesis. S.V. Rao acknowledges financial support from CSIR, India.

References

[1] Mirkin, C.A.; Letsinger, R.L.; Mucic, R.C.; Storhoff, J.J. *Nature* **1996,** *382,* 607–609.
[2] Gracias, D.H.; Tien, J.; Breen, T.L.; Hsu, C.; Whitesides, G.M. *Science* **2000,** *289,* 1170–1172.
[3] Han, G.; Ghosh, P.; De, M.; Rotello, V.M. *Nanobiotechnology* **2007,** *3,* 40–45.
[4] Wang, L.; Li, J.; Song, S.; Li, D.; Fan, C. *J. Phys. D: Appl. Phys.* **2009,** *42,* 203001.
[5] Qian, X.; Peng, X.H.; Ansari, D.O.; Yin-Goen, Q.; Chen, G.Z.; Shin, D.M.; Yang, L.; Young, A.N.; Wang, M.D.; Nie, S. *Nat. Biotechnol.* **2008,** *26,* 83–90.
[6] Sharverdi, A.R.; Mianaeian, S.; Shahverdi, H.R.; Jamalifar, H.; Nohi, A.A. *Process Biochem.* **2007,** *42,* 919–923.
[7] Ahmad, A.; Senapati, S.; Khan, M.I.; Kumar, R.; Sastry, M. *Langmuir* **2003,** *19,* 3550–3553.
[8] Nair, B.; Pradeep, T. *Cryst. Growth Des.* **2002,** *2,* 293–298.
[9] Ahmad, A.; Mukherjee, P.; Senapati, S.; Mandal, D.; Khan, M.I.; Kumar, R.; Sastry, M. *Colloids Surf., B* **2003,** *28,* 313–318.
[10] Shiv Shankar, S.; Ahmad, A.; Pasricha, R.; Sastry, M. *J. Mater. Chem.* **2003,** *13,* 1822–1826.
[11] Philip, D. *Spectrochim. Acta A* **2009,** *73,* 374–381.

[12] Badri Narayanan, K.; Sakthivel, N. *Mater. Lett.* **2008,** *62,* 4588–4590.
[13] Song, J.Y.; Jang, H.K.; Kim, B.S. *Process Biochem.* **2009,** *44,* 1133–1138.
[14] Sathyavathi, R.; Krishna, M.B.; Venugopal Rao, S.; Saritha, R.; Narayan Rao, D. *Adv. Sci. Lett.* **2010,** *3,* 138–143.
[15] Sathyavathi, R.; Krishna, M.B.; Narayana Rao, D. *J. Nanosci. Nanotechnol.* **2011,** *11,* 2031–2035.
[16] Chang, Q.; Ye, H.; Song, Y. *Colloids Surf., A* **2007,** *298,* 58–62.
[17] Lee, Y.H.; Yan, Y.; Lakshminarayana, P.; Xua, Q.H. *Appl. Phys. Lett.* **2009,** *95,* 023105.
[18] Ros, I.; Schiavuta, P.; Mattei, G.; Bozio, R. *Proc. SPIE* **2009,** *7394,* 739412.
[19] De Boni, L.; Wood, E.L.; Toro, C.; Hernandez, F.E. *Plasmonics* **2008,** *3,* 171–176.
[20] Li, C.; Jiang, L.; Liu, H.; Li, Y.; Song, Y. *Chem. Phys. Chem.* **2009,** *10,* 2058–2065.
[21] Philip, R.; Kumar, G.R.; Sandhyarani, N.; Pradeep, T. *Phys. Rev. B* **2000,** *62,* 13160–13166.
[22] Elim, H.I.; Yang, J.; Lee, J.Y.; Mi, J.; Ji, W. *Appl. Phys. Lett.* **2006,** *88,* 083107.
[23] Shen, H.; Cheng, B.L.; Lu, G.W.; Guan, D.Y.; Chen, Z.H.; Yang, G.Z. *J. Phys. D: Appl. Phys.* **2006,** *39,* 233–236.
[24] Wang, W.; Sun, W. *J. Phys. Chem. B* **2006,** *110,* 20901–20905.
[25] Couris, S. Presented at the ICTON Mediterranean Winter Conference, Sousse, Tunisia, Dec 6–8, 2007; Paper Th2A.1.
[26] Zhan, C.; Li, D.; Zhang, D.; Xu, W.; Nie, Y.; Zhu, D. *Opt. Mater.* **2004,** *26,* 11–15.
[27] Sheik-Bahae, M.; Said, A.A.; Wei, T.; Hagan, D.J.; Van Stryland, E.W. *IEEE J. Quantum Electron.* **1990,** *26,* 760–769.
[28] Venkartam, N.; Narayana Rao, D.; Giribabu, L.; Venugopal Rao, S. *Appl. Phys. B* **2008,** *91,* 149–156.
[29] Polavarapu, L.; Venkatram, N.; Wei, J.; Xu, Q.-H. *Appl. Mater. Interfaces* **2009,** *1,* 2298–2303.
[30] Souza, R.F.; Alencar, M.A.R.C.; da Silva, E.C.; Meneghetti, M.R.; Hickmann, J.M. *Appl. Phys. Lett.* **2008,** *92,* 201902.
[31] Francois, L.; Mostafavi, M.; Belloni, J.; Delouis, J.F.; Delaire, J.; Feneyrou, P. *J. Phys. Chem. B* **2000,** *104,* 6133–6137.
[32] Lv, J.; Jiang, L.; Li, C.; Liu, X.; Yuan, M.; Xu, J.; Zhou, W.; Song, Y.; Liu, H.; Li, Y.; Zhu, D. *Langmuir* **2008,** *24,* 8297–8302.
[33] Kai, W.; Hua, L.; Ming, Fu, F.; Guang, Y.; Pei-Xiang, L. *Chin. Phys. Lett.* **2010,** *27,* 124204.
[34] Wang, K.; Long, H.; Fu, M.; Yang, G.; Lu, P. *Opt. Express* **2010,** *18,* 13874–13879.
[35] Cui, F.; Hua, Z.; Wei, C.; Li, J.; Gao, Z.; Shi, J. *J. Mater. Chem.* **2009,** *19,* 7632–7637.